

Grasping Polyhedral Objects with Slip

Swaminathan Gopalswamy
Dept. of Mech. Eng
Univ. of California
Berkeley, CA 94720R.S. Fearing
Dept. of EE&CS
Univ. of California
Berkeley, CA 94720

Abstract

A force strategy developed by Fearing [1986b], for automatically grasping two dimensional polygonal objects with a dextrous hand with point contact with friction is shown to be applicable to three dimensional polyhedral objects. The algorithm essentially consists of position control of one finger and force control of the other along the *internal force directions*. Basic geometric constraints on the object are obtained for feasible grasping with two fingers. It is observed that when an object is rotated about the line passing through soft finger contacts, the fingers slip on the object in a simple predictable trajectory.

1 Introduction

The dexterity required for many assembly operations is not met by parallel-jaw type hands. To meet this need, various dextrous hands have been developed, e.g. Salisbury [1982] and Jacobsen et al [1985]. Most proposed grasping algorithms for these hands require detailed knowledge of the object's shape, location, and orientation. A grasp acquisition algorithm is a method of controlling the fingers which leads to a stable grasp of the object. A grasp is defined as stable if the object is in equilibrium and there is no slip any of the fingers.

The use of sliding in manipulation tasks was promoted by the 1982 work of Mason [1986] and later by Peshkin [1986, 1987]. An algorithm for automatic stable grasping of polygonal objects, in the absence of local information, with two fingers with point contact with friction was developed by Fearing [1986]. The central idea was to squeeze along the internal force directions. That paper shows how the object motion occurs upon such grasping, starting from any initial condition, and determines the geometric constraint on the polygonal object that has to be satisfied for a stable grasp. An automatic grasping technique based on pushing with line contacts is discussed by Brost [1986]. Trinkle [1988] looked at grasp acquisition while lifting objects against gravity. Brock [1988] discusses reducing grasp constraints to allow slipping in preferred directions.

To constrain an object we need six independent forces. Each finger, if point contact with friction is assumed, can produce three forces, with the constraint that the normal force is always positive, and the force is within the friction cone. If enough friction force can be achieved (by, for instance, increasing the internal forces), and if the object is convex, then with two fingers we can counter any force/moment except the moment about the line passing through the contact points. If we assume soft fingers, even this restriction is removed. (Soft fingers [Salisbury and Craig, 1982] can in addition resist a moment about the axis between two fingers. Thus two soft fingers can completely restrain the object.)

The precondition for achieving any frictional force is that the internal force lie *within* the friction cone. If rotation of the object occurs during squeezing, then the internal force will lie *on* the friction cone. Then there will be a certain amount of slipping before any external force can be resisted. This is discussed in section 3.

It is worthwhile to determine the geometric constraints that have to be satisfied to acquire any object into a grasp. This is done for the case of two fingers with point contact friction for polygonal objects in [Fearing 1986b]. In the present paper that constraint is shown to be valid for convex polyhedral objects as well. If the surface normals at contacts form an angle less than or equal to twice the friction cone angle the object *can* be acquired and grasped with only two fingers. It is intuitively apparent that with more fingers this constraint will be relaxed. Extra fingers are costly, so it behooves us to study acquisition with the minimum number. Extra fingers can be used for regrasping.

Section 2 analyses the behaviour of the object under the internal-force-algorithm. **Section 3** explains limiting or marginal stability of the resulting grasp. **Section 4** describes the phenomenon of fingers *walking about*, as a polyhedron is rotated in a two finger grasp.

2 The Grasp Acquisition Method

2.1 Nomenclature and representation

We denote the normal to the surface at finger 1 by \hat{n}_1 and that at finger 2 by $-\hat{n}_2$. (The unit vector at the second finger is directed into the object- this simplifies the geometry). The unit vector along the line from finger 2 to finger 1 is denoted by \hat{r} . The directions of the forces on the object at finger 1 and finger 2, respectively, are $-\hat{f}_1$ and $+\hat{f}_2$.

The angle between \hat{r} and \hat{n}_i is α_i , where $i = 1, 2$ is the finger number. ψ is the angle between \hat{n}_1 and \hat{n}_2 , which is the angle between the two contacting surfaces. It is a constant for polyhedral objects during the grasping operation as long as the contacts remain on the same faces. The friction cone angle is denoted by ϕ_s . For simplicity the difference between kinetic and static friction coefficients is neglected. The angle between \hat{f}_i and \hat{n}_i is γ_i . Because the forces on the object must be within or at the edge of the friction cone, $\gamma_1, \gamma_2 \leq \phi_s$ always.

In this paper the analysis is done geometrically, using spherical triangles to represent angles between unit vectors — Lakshminarayana [1976]. In this representation the direction of a unit vector is mapped to its corresponding point on a unit sphere. The point on the surface is the location where a unit vector at the origin intersects the surface of the sphere. (For example, \hat{z} is mapped to the north pole of the sphere). The angle between two

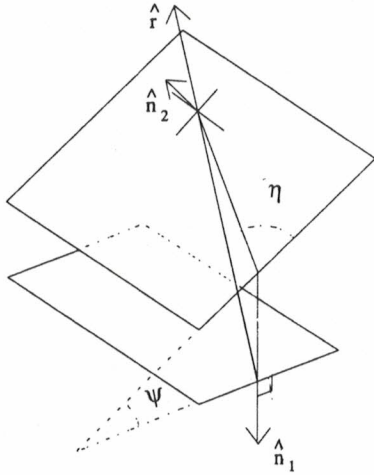


Figure 1: Polyhedral Representation

ψ is the angle between the two faces, and η is the skew of the line between the fingers from the polygonal case.

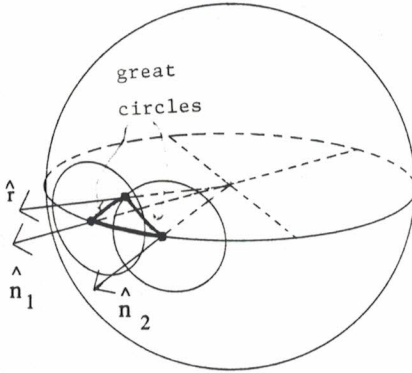


Figure 2: Spherical Triangle Representation

Great circles connect points (representing directions) on the surface of the unit sphere.

vectors is represented by the arc of the great circle containing the two vector ends (Figure 2).

2.2 Graspability

For any stable grasp we need equilibrium of forces and moments. This necessitates that the forces be equal and opposite, and that the lines of action of the forces coincide (Figure 3a). i.e. $\hat{\mathbf{f}}_1 = \hat{\mathbf{f}}_2 = \hat{\mathbf{r}}$. Thus $\alpha_1 = \gamma_1$, and $\alpha_2 = \gamma_2$ at equilibrium.

Now for a stable grasp $\alpha_1, \gamma_1, \alpha_2$ and $\gamma_2 \leq \phi_s$, (i.e. $\hat{\mathbf{f}}_2 \cdot \hat{\mathbf{n}}_2 \leq \cos \phi_s$.) Graphically this restricts the location of $\hat{\mathbf{r}}$ to within the shaded area shown in Figure 3b. It shows spherical circles of spherical radius ϕ_s .

As ψ increases, for a given ϕ_s , the shaded region (the possible directions of $\hat{\mathbf{r}}$ for stable grasping) decreases, and in the limit vanishes. This limit for ψ is obtained when the two spherical circles touch each other, wherein we obtain $\psi_{max} = 2\phi_s$.

This can be shown rigorously using the spherical triangle formulae developed by Lakshminarayana [1976]. We denote the angle

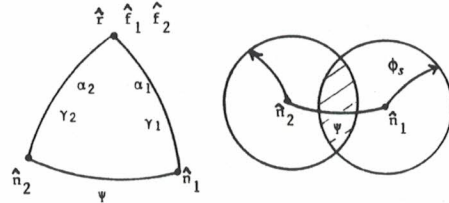


Figure 3: Spherical Triangle for Stable Grasp

a. Finger forces are coincident with the line between the two fingers. b. Range of $\hat{\mathbf{r}}$ for no sliding is shown in the shaded region.

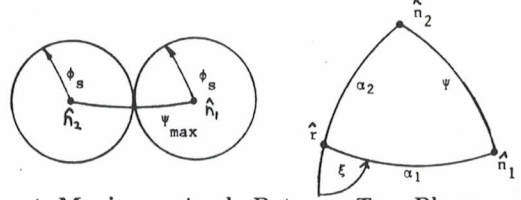


Figure 4: Maximum Angle Between Two Planes

At the limiting angle, ψ_{max} , the object can barely be grasped.

between the plane of $(\hat{\mathbf{n}}_2, \hat{\mathbf{r}})$ and $(\hat{\mathbf{r}}, \hat{\mathbf{n}}_1)$ as ξ . Then we have

$$\cos \psi = \cos \alpha_1 \cos \alpha_2 - \sin \alpha_1 \sin \alpha_2 \cos \xi$$

For a stable grasp α_1 and $\alpha_2 \leq \phi_s \leq 90$ deg. Therefore $\cos \alpha_1, \cos \alpha_2, \sin \alpha_1$ and $\sin \alpha_2 \geq 0$. ψ is maximized when $\cos \psi$ is minimized. Considering the first term we see that $\cos \alpha_1 \cos \alpha_2$ is minimum when $\alpha_1 = \alpha_{1max} = \phi_s$, and similarly $\alpha_2 = \alpha_{2max} = \phi_s$. This also maximizes the $\sin \alpha_1 \sin \alpha_2$ part of the second term. The only variable is ξ . For any given ξ , we have maximum ψ given by

$$\cos \psi_{max} |_{\xi} = \cos^2 \phi_s - \sin^2 \phi_s \cos \xi \pm \sin^2 \phi_s$$

$$\cos \psi_{max} |_{\xi} = \cos 2\phi_s + \sin^2 \phi_s (1 - \cos \xi)$$

Thus ψ_{max} , over all ξ is obtained when $1 - \cos \xi$ is minimum, i.e. $\xi = 0$, wherein we get

$$\psi_{max} = 2\phi_s$$

Thus the graspability condition for a polyhedral object with two fingers with point contact with friction is that the angle between the two contacted planes be less than or equal to twice the friction cone angle. (Also shown by [Nguyen 1987] for two soft fingers).

It is also to be noted that at the maximum angle between planes, $\hat{\mathbf{r}}$ is forced to be on the spherical line from $\hat{\mathbf{n}}_1$ to $\hat{\mathbf{n}}_2$ — that is $\hat{\mathbf{r}}, \hat{\mathbf{n}}_1$ and $\hat{\mathbf{n}}_2$ are in a plane as in the polygonal case.

2.3 Grasp Forces

We shall consider only those objects that are *graspable* as defined in Section 2.2. We now apply the algorithm proposed by Fearing 1986a : assuming that finger 1 has a controllable stiffness, we write the force at finger 1, in spherical coordinates, as:

$$\vec{\mathbf{F}}_1 = \begin{bmatrix} F_{r0} + k_r(\Delta r) \\ k_{\theta r} \sin \phi(\Delta \theta) \\ k_{\phi r}(\Delta \phi) \end{bmatrix}$$

where r, θ, ϕ are the spherical coordinates of finger 1 with respect to finger 2 which is at the origin. We set $k_{\theta}, k_{\phi} \rightarrow \infty$, and $k_r \rightarrow 0$. Thus the line of action of the fingers does not change during grasping, that is the $\hat{\mathbf{r}}$ in the spherical triangle representation remains fixed. The object, however, moves, and hence so do $\hat{\mathbf{n}}_1$ and $\hat{\mathbf{n}}_2$. Note that finger 2 is fixed in space, thus the force at

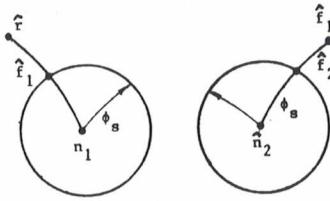


Figure 5: Forces for Slipping at Finger 1

a. Reaction force at finger 1. b. Reaction force at finger 2, on edge of friction cone. If finger 1 is *not* slipping, \hat{f}_1 would be inside the small circle representing the friction cone.

finger 2 is due only to the reaction force arising out of the position constraint.

We first identify the relative positions of \hat{r} with respect to the normals for the three cases of no slip at both fingers, slip at one finger alone, or slip at both fingers. These cases of slip or sticking at fingers are determined by reaction forces produced when applying a force at finger one alone.

2.3.1 Reaction force at finger 1 and finger 2

If finger 1 is slipping, the direction of the force on the object at finger 1 (\hat{f}_1) is on the edge of the friction cone, represented as the small circle of spherical radius ϕ_s with \hat{n}_1 as its center. In other words, \hat{f}_1 lies in the plane of \hat{r} and \hat{n}_1 represented by the great circle through \hat{r} and \hat{n}_1 . Thus the location of \hat{f}_1 is on the intersection of the two circles (Figure 5a).

For equilibrium, the reaction force at finger 2 will be in the \hat{f}_1 direction (direction of force at finger 1). Thus \hat{f}_2 lies in the plane of \hat{f}_1 and \hat{n}_2 , represented by the great circle arc from \hat{n}_2 to \hat{f}_1 in Figure 5b.

2.4 Which Fingers Slide?

We can now identify the regions of \hat{r} where we would have slip at a finger. In Figure 6, the shaded region shows the allowed directions of \hat{r} for the 4 slip combinations. The regions are referred to by the corresponding letter label.

Note that region B, that is slip at finger 1 alone, does not include the whole friction cone at finger 2. Because \hat{f}_1 is slipping, \hat{f}_1 will be on the edge of its friction cone, not pointed along \hat{r} . The force at finger 2, \hat{f}_2 is a reaction force, which must be on a great circle between \hat{f}_1 and \hat{n}_2 , and inside the friction cone at the second finger.

Now we consider the behavior of the object with each of the regions as the starting region. In the analysis we assume quasi-static behavior of the object.

2.4.1 No Slip (Starting from region A)

This is the trivial case when we start in a stable grasp right away. Both finger forces are within the friction cone.

2.4.2 Slip at Finger One (Starting from region B)

In this section we have equilibrium of forces, though not moments, i.e. \hat{f}_1 and \hat{f}_2 are the same, but not colinear. (\hat{f}_1 is at the intersection of the great circle from \hat{n}_1 to \hat{r} with the friction cone circle. This intersection point gives the instantaneous direction for sliding. \hat{f}_2 is a reaction force that will be opposite in direction from \hat{f}_1 for quasi-static equilibrium, and thus at the same point on the unit sphere). For sliding at finger 1, the force angles $\gamma_1 = \phi_s$ and $\gamma_2 = \text{some } \gamma \leq \phi_s$ —Figure 7b. We note that the moment about finger 2 is perpendicular to the plane of \hat{r} and \hat{n}_1 . This tends to

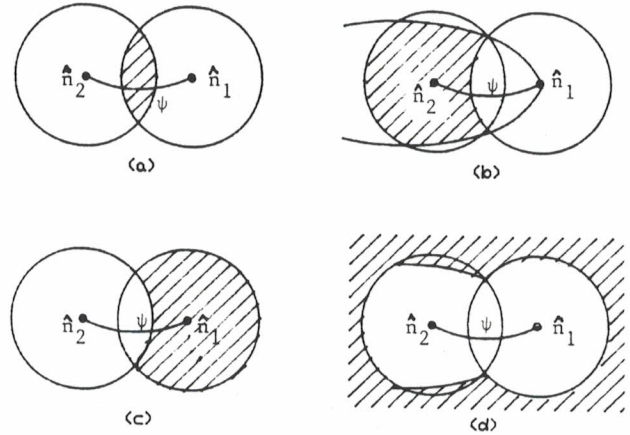


Figure 6: Location of \hat{r} for Slip

a. region A: no slip at both fingers. b. Region B: slip at finger 1 alone. c. Region C: slip at finger 2 alone. d. Region D: slip at both fingers. The boundary lines in b. are great circles passing through \hat{n}_1 and the intersections of the two small circles of spherical radii ϕ_s .

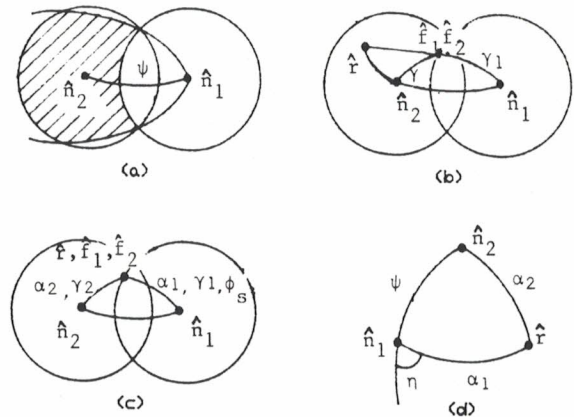


Figure 7: Rotation of Object Being Grasped with Slip at Finger 1

a. For slipping at finger 1 but not Finger 2, force must be on edge of friction cone, in region B. b. As finger 1 slips, \hat{r} rotates along great circle towards \hat{f}_1 point. c. Final grasp. d. Spherical triangle representation.

rotate the object so that \hat{f}_1, \hat{f}_2 coincide with \hat{f} . Every point on the spherical line between \hat{n}_1 and \hat{n}_2 moves along circles containing the point and parallel to the great circle containing \hat{f} and \hat{n}_1 . In fact, the spherical triangle of \hat{n}_2, \hat{n}_1 and \hat{f} rotates as a whole, to align \hat{f} with \hat{f} . The final position is shown in Figure 7c.

Denoting the angle between the plane of \hat{f}, \hat{n}_1 and \hat{n}_1, \hat{n}_2 by η as in Figure 7d, spherical triangle solutions give

$$\hat{n}_2 \cdot \hat{f} = \cos \alpha_2 = \cos \alpha_1 \cos \psi - \sin \alpha_1 \sin \psi \cos \eta \quad (1)$$

At the final position, the force at finger 1 will be at the edge of the friction cone, (with $\alpha_1 = \gamma_1 = \phi_s$), and the force at finger two is

$$\cos \gamma_2 = \cos \phi_s \cos \psi - \sin \phi_s \sin \psi \cos \eta \quad (2)$$

If we write $\alpha_1' = \alpha_1 - \beta$, where β is the rotation of the object about the axis ($\hat{f} \times \hat{n}_1$), α_1' is the instantaneous α_1 :

$$\cos \alpha_2' = \cos \alpha_1' \cos \psi - \sin \alpha_1' \sin \psi \cos \eta$$

simplifying,

$$\cos \alpha_2' = \cos \beta \cos \alpha_2 + c_1 \sin \beta$$

where $c_1 = \sin \alpha_1 \cos \psi + \cos \alpha_1 \sin \psi \cos \eta = a \text{ constant}$. c_1 is a constant because η does not change during rotation. Thus

$$\cos \alpha_2' = \cos(\delta - \beta) \sqrt{\cos^2 \psi + \sin^2 \psi \cos^2 \eta}$$

, where $\tan \delta = c_1 / \cos \alpha_2$

We note that the relation between α_2' and β is not linear except for $\eta = 0$, the case of a polygon as shown in [Fearing 86].

2.4.3 Slip at Finger 2 (Region C)

With slip at finger 2, there will be a moment in the (\hat{f}, \hat{n}_2) plane. Since there is no slip at finger 1, it must be the rotation center. The rotation about finger 1 brings \hat{f} closer to the friction cone about \hat{n}_2 .

2.4.4 Slip at Both Fingers (D)

Only a geometric analysis of the behavior is presented here as the equations become complex. We first note that the forces at the two fingers cannot be equal (because the reaction force at Finger 2 is outside the friction cone), and thus we have nonequilibrium of forces and moments. Thus \hat{f}_1 and \hat{f}_2 are distinct. Therefore we have two components of the moments. One is perpendicular to the plane of (\hat{f}, \hat{n}_1), and the other is perpendicular to the plane of (\hat{n}_2, \hat{f}_1)—Figure 8. The first moment tends to rotate the object so that \hat{f}_1 moves towards \hat{f} , while the second moment tends to rotate \hat{f}_2 such that it moves towards \hat{f}_1 . Depending on the relative weights of the two component moments we would end up in either region A, B, or C. From region B or C we would eventually end up in the desired region A as discussed previously.

Once slip stops at one finger, the acquisition will not return to the two finger sliding case. The trajectory taken by \hat{f} will depend heavily on the stiffness and friction properties of the fingers. The important consideration is the endpoints, that is whether the object will become securely grasped. The acquisition will be successful if $\psi \leq 2\phi_s$.

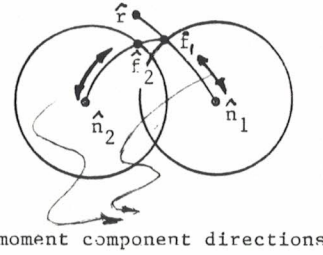


Figure 8: Rotation with Slip at Both Fingers

3 Marginal Stability

What is the ability of the grasp resulting from the squeezing algorithm to resist external forces and moments? Except when the starting grasp is stable, the grasp acquisition ends up with \hat{f} being aligned with the friction cone at finger 1 (neglecting dynamic effects). With one finger force at the edge of the friction cone, a moment that pushes the force outside the friction cone can not be resisted. Thus not all external forces can be resisted by simply increasing the internal force. (In our case we need to increase the radial force, or k_r).

However this is not as serious as it seems to be. Whenever there is an external force / moment that produces a reaction that is outside the friction cone at any finger, there is sliding at that finger. If the disturbance force is of a limited magnitude, the resulting rotation of the object brings the reaction force back into the friction cone. Thus if a certain amount of slipping at the fingers is acceptable we would be able to resist external forces / moments other than the moment about \hat{f} . It is because of this slipping that we call this grasp *marginally stable*. If the disturbance force is removed, the object will rotate back to a stable grasp, probably in a new position.

Thus the squeezing algorithm is sufficient to achieve a stable grasp of polyhedral objects, in the absence of disturbance forces, as long as the geometric constraint is satisfied, ie $\psi \leq 2\phi_s$. With truncated vertices, it is possible for the fingers to slip totally off the sides and touch each other. When that is recognized — based on, for instance, a threshold for the distance between the two fingers, we would need to start over again with a different initial grasp.)

By increasing the radial force arbitrarily any external force can be taken care of — the marginal stability is ensured if a small amount of further slipping can be tolerated.

4 Slip during Yaw Motion

Fearing[1986a] mentioned object rotation relative to the fingers about the line passing through the contact points, a so called *yaw* motion. With point contacts one foresees no problem in this — we use the a third finger to provide the turning moment. However, in practice it is difficult to have a point contact. Therefore we examine the effect of soft fingers on the yawing motion.

The stable grasp algorithm with point contacts is applicable with soft fingers if the area of contact is not unreasonably large. The rotation about \hat{f} , however, is interesting. If the object is rotated, the fingers slip and translate on the object. The direction of the translation depends on the force applied to cause rotation of the object. An intuitive explanation is given for this *walking about* of the fingers on the object follows.

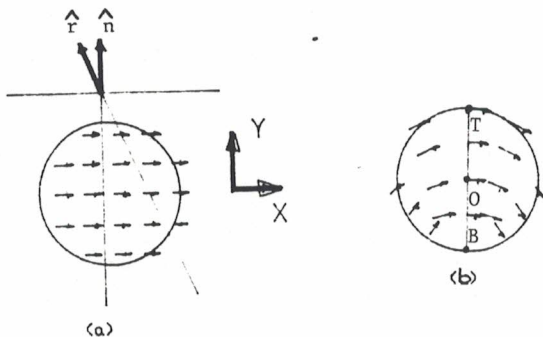


Figure 9: Contact Tangential Stress Assumptions

The figure shows the tangential stress distribution on the object due to: a. Radial force, the force being directed into the object. b. Superposition of the rotational and tangential stress fields.

4.1 Soft finger contact

A soft finger tends to assume the shape of the contacting surface. If we have a spherical finger tip the area of contact will be a circle on the planar surface of the object by Hertzian contact modelling. If we have only a normal force, by symmetry we have a circular contact. When there is a tangential force there might be a skew in the circle, but we neglect it here (the actual nature of the contact would require a very complicated elastic analysis).

The soft finger is made, in general, of a material like rubber. For ease of analysis we will assume a constant pressure distribution on the contact. This constant pressure hypothesis is called the very-soft-finger approximation [Howe et al 1988].

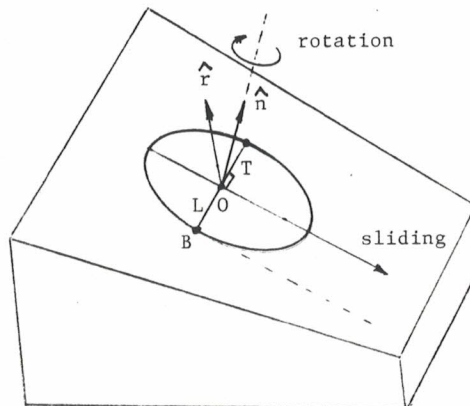
Consider a polyhedron grasped with two soft fingers. We assume Coulomb friction, thus we have a uniform tangential stress in the direction of \hat{f} in the plane of the contact. (The exact distribution is again a complicated elasticity problem).

Consider a single soft finger tip pressed against a plane. When a pure torque is applied by the finger, the resulting tangential stress is distributed symmetrically about the contact radius, and proportional to the distance from the center of contact. (The tangential stress could be considered proportional to the virtual displacement about the rotation center). This is true when there is no slip. However, once slip starts the stress becomes constant and equal to the shear slip limit μ_{slip} , and starting from the circumference of the contact circle the slip region progresses towards the center of contact, until the magnitude of the stress becomes the same ($= \mu_{slip}$) throughout the contact area [Cutkosky and Wright, 1986].

4.2 The Contact Trajectory

When the normal force, the tangential force, and the applied torque act together, we superimpose the effect of each of these to obtain the combined effect. (This is a coupled shear and moment assumption. See Jameson [1985] and Howe et al [1988] for more accurate approximations). Without loss of generality, we shall analyze the case when stress due to the pure radial force is along the positive X direction (as in Figure 9a). From the superposed stress distribution (Fig. 9b) we see that the bottom most point (B) has the minimum tangential stress and the top most point (T) has the maximum tangential stress. If there is relative rotation, the rotation center has the minimum tangential stress, and all the other points have stress in directions perpendicular to

Figure 10: Rotation of Object Grasped with Soft Fingers. The fingers slide down the object as it rotates.



the radius from the rotation center.

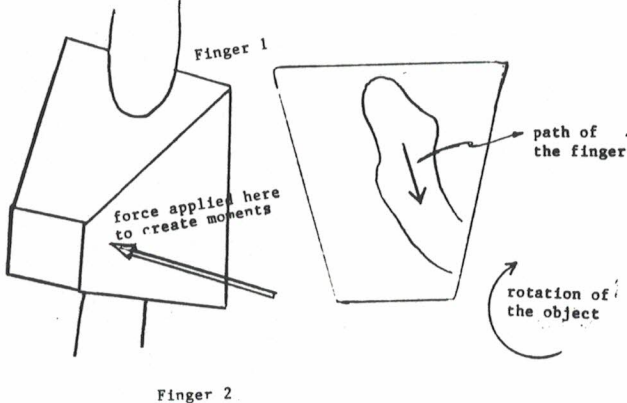
We observe that by superposition we have the center of rotation to be on the line perpendicular to the plane of \hat{f} and \hat{n} . Let us call the line L . The rotation center can not be outside the contact circle because if it were, it would imply that all the points on the line L inside the contact circle are slipping. For all points on L to slip, they would need to have a tangential stress greater than what they had before the pure torque was applied. But that is not possible because we started with the tangential stress at all points within the friction cone (a stable grasp), and the addition of a pure torque about the center of contact can not add tangential stress in the same direction throughout the line L .

The exact location of the center of rotation within the circle needs a more elaborate analysis, which is not attempted here. We will assume a worst case condition, that is, the instantaneous rotation center at the edge of the circle of contact. Future elastic analysis should be done to determine the location more exactly. Let us look into the equation of motion of the center of the finger with respect to the surface of the object. 'O', the center of the circle of contact, rotates at every instant about the point B , defined by the intersection of the line L and the circle of contact. L itself is defined as the line on the surface of contact and passing through O and perpendicular to the plane of \hat{f} and \hat{n} . In a stable grasp, without the presence of disturbance forces, $\hat{f} = \hat{r}$, and hence L is just perpendicular to the plane of \hat{f} and \hat{n} . This is kinematically equivalent to a circle rolling on a straight line parallel to the plane of \hat{f} and \hat{n} , at a distance equal to the radius of contact. (Fig. 10). Thus as the object rotates, the fingers have net slip down the slope of the polyhedron. (This is kinematically equivalent to rotation about the center of contact and a tangential slip, effectively due to a reduced tangential coefficient of friction when a moment is applied [Howe et al 1988]).

Now in practice if we use the third finger to apply a torque we also have a disturbance force. This disturbance force causes the direction of \hat{f} and \hat{r} to differ and therefore we get a line that is not parallel to the plane of \hat{f} and \hat{n} . The deviation depends upon the force applied by the third finger. As the moment required to cause rotation is fairly constant for a constant normal force, the location of the third finger assumes importance.

We notice in experiments that the first finger travels towards the third finger, with increasing slip as it nears the third finger (that is, as the moment arm becomes shorter). Thus we have the

Figure 11: **Sliding Trajectory with Two human Fingers**
Results from preliminary experiment, as pyramid is rotated, fingers slid on surface in pattern shown. Fingers were coated with copy machine toner.



walking about of the fingers on the object. An initial experiment with a human grasping a truncated pyramid gave rise to an interesting pattern of finger sliding and rotation along the object surface. See Figure 11. Since a varying magnitude force and not a pure torque was applied, the trajectory is not a straight line.

5 Conclusions and Discussions

The *grasp acquisition algorithm* proposed by Fearing[1986] for polygonal objects seems to be a *natural grasping algorithm*, where the same algorithm results in a grasp which can resist external disturbances. This algorithm was examined with respect to polyhedral objects, and is valid when sides adjoin or are long enough such that fingers don't slip off, and the angle between faces is less than twice the friction angle.

The manipulations such as rolling that were discussed for the polygonal case [Fearing 1986a] have not yet been analyzed for three dimensional objects. However it is expected that the flavor of the analysis should be the same.

Rotation of the object about the axis between two fingers, the yaw motion, was discussed. This led to the observation that the fingers *walk about* on the object if soft fingers are used. In this paper, an intuitive explanation of the phenomenon is given, which agrees reasonably with experiments.

There were quite a few assumptions made to preserve the simplicity of the analysis. First of all, we had the quasi-static behavior assumption. Though this assumption is pretty much in vogue, future work may remove this assumption advantageously. Similarly, the uniform pressure distribution under the very soft finger assumption is quite inaccurate. A more elaborate elastic/plastic analysis of the fingers could be made.

In this paper, a step has been made towards stable acquisition and manipulation of polyhedral objects with minimum number of fingers and minimum sensory information.

Acknowledgements

The authors would like to thank Rob Howe for helpful comments.

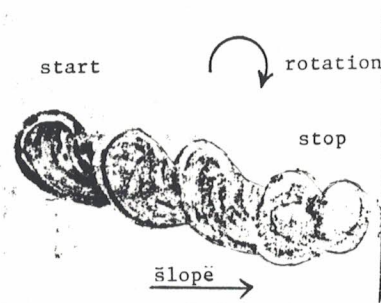


Figure 12: **Sliding Trajectory on 20 degrees Plane**
An approximate pure moment is applied by hand, as object is grasped with two circular rubber grommets.

6 References

- D. L. Brock, "Enhancing the Dexterity of a Robot Hand using Controlled Slip", IEEE ICRA, Philadelphia, April, 1988.
- R.C. Brost, "Automatic Grasp Planning in the Presence of Uncertainty", IEEE Int. Conf. on Robotics and Automation, San Francisco, CA April 1986.
- M. R. Cutkosky, P. K. Wright, "Friction, Stability and the Design of Robotic fingers", *Int. Jnl. of Rob. Res.*, Vol.5, No.4, Winter 1986.
- R. S. Fearing, "Implementing a force strategy for object re-orientation", IEEE Int. Conf. on Robotics and Autom. San Francisco, CA, April 1986.
- R. S. Fearing, "Simplified Grasping and manipulation with dextrous robot hands", *IEEE J. of Rob. and Autom.*, Vol RA-2, No. 4, Dec 1986 b.
- R.D. Howe, I. Kao, M.R. Cutkosky, "The Sliding of Robot Fingers Under Combined Torsion and Shear Loading", IEEE Intern. Conf. on Robotics and Automation, Philadelphia, PA April 1988.
- S.C. Jacobsen, J. E. Wood, D. F. Knutti, K. B. Biggers and E. K. Iversen, "The version I Utah/MIT dextrous hand", in *Robotics*, H. Hanafusa and H. Inone, Eds., Cambridge, MA:MIT 1985.
- J. W. Jameson, "Analytic Techniques for Automated Grasp", Ph.D. Dissertation, Stanford University, June 1985.
- K. Lakshminarayana, "An approach to the Displacement Analysis of Spatial Mechanisms — I", *Mechanism and Machine Theory*, 1976, Vol 11, p381.
- M.T. Mason, "Mechanics and planning of Manipulator Pushing Operations", *Int. J. of Rob. Res.*, Vol.5, No.3, Fall 1986.
- V. Nguyen, "Constructing Force Closure Grasps in 3 dimensions", IEEE ICRA, Raleigh, NC 1987.
- M. A. Peshkin and A. C. Sanderson, "Manipulation of a Sliding Object", IEEE ICRA, San Francisco CA, April 1986.
- M. A. Peshkin and A. C. Sanderson, "Planning robotic manipulation strategies for sliding objects", IEEE ICRA, Raleigh, NC, April 1987.
- J.K. Salisbury and J.J. Craig, "Articulated Hands: Force Control and Kinematic Issues," *Int. Jnl. of Rob. Res.* vol. 1, no. 1, Spring 1982.
- J. C. Trinkle, "Grasp Acquisition Using Liftability Regions", IEEE ICRA, Philadelphia, April, 1988.